ORGANOMETALLICS Article
Cite This: Organometallics XXXX, XXX, XXX−XXX
pubs.acs.org/Organometallics

Synthesis and Reactivity of Metal−Ligand Cooperative Bifunctional Ruthenium Hydride Complexes: Active Catalysts for β-Alkylation of Secondary Alcohols with Primary Alcohols

Jing Shi,[†] Bowen Hu,[†] Peng Ren,[‡] Shu Shang,[†] Xinzheng Yang,*[,§,∥] and Dafa Chen*[,†]

[†]MIIT Key Laboratory of Critical Materials Technology for New Energy Conversion and Storage, School of Chemistry and Chemical Engineering, Harbin Institute of Technology, Harbin 150001, People's Republic of China

[‡]School of Science, Harbin Institute of Technology (Shenzhen), Shenzhen 518055, People's Republic of China

[§]Beijing National Laboratory for Molecular Sciences, State Key Laboratory for Structural Chemistry of Unstable and Stable Species, CAS Research/Education Center for Excellence in Molecular Sciences, Institute of Chemistry, Chinese Academy of Sciences, Beijing 100190, People's Republic of China

[∥]University of Chinese Academy of Sciences, Beijing 100049, People's Republic of China

Supporting Information

ABSTRACT: Three unsymmetrical NNN ligands with a 2-hydroxypyridyl fragment were used to react with RuHCl(PPh$_3$)$_3$(CO), affording the three bidentate ruthenium hydride complexes [(R$_1$-C$_5$H$_3$N-CH$_2$-C$_5$H$_3$N-C$_5$H$_3$N-R$_2$)RuH(PPh$_3$)$_2$(CO)][Cl] (R$_1$ = R$_2$ = OH, **2a**; R$_1$ = OH, R$_2$ = H, **2b**; R$_1$ = H, R$_2$ = OH, **2c**), respectively. When **2a**,**b** were treated with *t*-BuOK, the two tridentate products [(O-C$_5$H$_3$N-CH$_2$-C$_5$H$_3$N-C$_5$H$_3$N-R$_2$)RuH(PPh$_3$)(CO)] (R$_2$ = OH, **3a**; R$_2$ = H, **3b**) were obtained, via selective deprotonation of the −OH group of PyCH$_2$PyOH moiety, indicating that this −OH group is more acidic than that of the PyPyOH moiety. The reaction of **2c** with *t*-BuOK generated the bidentate product [(C$_5$H$_4$N-CH$_2$-C$_5$H$_3$N-C$_5$H$_3$N-O)RuH(PPh$_3$)$_2$(CO)] (**3c**) and the tridentate product [(C$_5$H$_4$N-CH$_2$-C$_5$H$_3$N-C$_5$H$_3$N-O)RuH(PPh$_3$)(CO)] (**3d**). **3d** could be further transformed to the diruthenium complex [(C$_5$H$_4$N-CH-C$_5$H$_3$N-C$_5$H$_3$N-O)Ru(PPh$_3$)(CO)]$_2$ (**3e**) via C−H activation of the −CH$_2$− group in boiling toluene. The catalytic activity for β-alkylation of secondary alcohols with primary alcohols of these eight ruthenium complexes was tested, and the bidentate complexes **2c** and **3c** exhibit the highest activity. Complex **3c** can be regarded as the intermediate of **2c**. These results are important for developing more efficient bifunctional catalysts for such reactions.

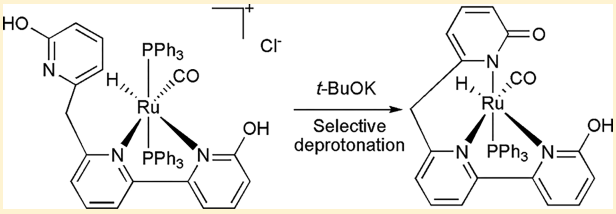

INTRODUCTION

Metal−ligand cooperative bifunctional complexes play crucial roles in chemical bond activation and catalysis.[1−21] A major strategy of designing metal−ligand cooperative catalysts is by introducing a proton-responsive ligand to the metal center. In the presence of a base, the proton-responsive site can be deprotonated, and the resulting complex might accept a proton from the substrate. The reversible structural changes of the ligand are beneficial for substrate activation. For example, many amido transition-metal complexes can promote H$_2$ activation and H$_2$-related catalytic reactions.[2−4] In addition, Milstein and other groups revealed that lutidine-based PNP-M and PNN-M complexes, which have slightly acidic methylene protons, exhibit interesting metal−ligand cooperation based on an aromatization−dearomatization process and have been exploited for a series of organic transformations.[5−7] Other types of metal−ligand cooperative complexes are transition-metal compounds with a 2-hydroxypyridyl group, which can be deprotonated to a pyridinol form with a C═O bond.[8−18]

Although there are various types of metal−ligand cooperative complexes, systems based on unsymmetric ligands with two or more proton-responsive sites are rare.[19−21] Ikariya and Kuwata et al. synthesized two ruthenium complexes based on NNC tridentate ligands containing a protic pyrazole and a N-heterocyclic carbene (Figure 1a,b) and studied their reactivity with bases. In both cases, the protic pyrazole ring was deprotonated first, indicating that the pyrazole was more acidic than the N-heterocyclic carbene.[20] Recently, the van der Vlugt

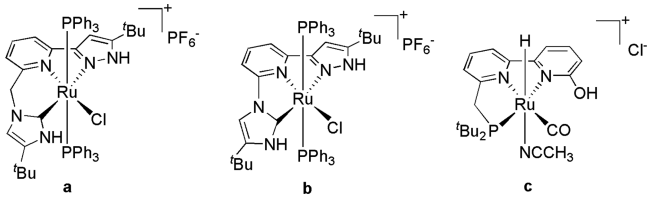

Figure 1. Ruthenium complexes **a**−**c** based on unsymmetric ligands with two proton-responsive sites.

Received: June 23, 2018

DOI: 10.1021/acs.organomet.8b00432
Organometallics XXXX, XXX, XXX−XXX

group developed a PNN ligand by the combination of 2-hydroxypyridyl and a PN fragment and introduced it to a ruthenium center (Figure 1c). Only the 2-hydroxypyridyl moiety was deprotonated to 2-pyridinol even with excessive DBU, demonstrating that the $-CH_2-$ protons were less acidic.[21c]

Recently, we have synthesized the ruthenium dichloride complexes **1a−c** based on the ligands [R_1-C_5H_3N-CH_2-C_5H_3N-C_5H_3N-R_2] (**L₁**, R_1 = OH, R_2 = OH; **L₂**, R_1 = OH, R_2 = H; **L₃**, R_1 = H, R_2 = OH) and studied their catalytic activity on transfer hydrogenation of ketones (Scheme 1).[22]

Scheme 1. Synthesis of Our Previous Ruthenium Complexes 1a−c[22]

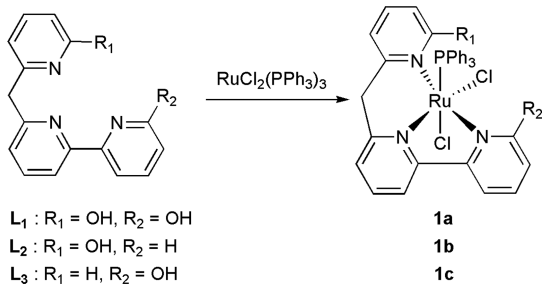

Complexes **1a−c** contain two or three proton-responsive sites (−OH and $-CH_2-$); however, their reactions with bases did not give any identified products. Herein, we report the synthesis of ruthenium hydride complexes supported by L_1−L_3 and their reactivity with base. Furthermore, these ruthenium complexes also showed high catalytic activity for *β*-alkylation of secondary alcohols with primary alcohols in air, which is regarded as an environmentally friendly method to synthesize *β*-alkylated alcohols and has been catalyzed by other ruthenium complexes.[17b,c,23,24]

RESULTS AND DISCUSSION

Synthesis and Characterization of Ru(II) Complexes. Reaction of **L₁** with $RuHCl(PPh_3)_3(CO)$ in refluxing methanol gave the product [(HO-C_5H_3N-CH_2-C_5H_3N-C_5H_3N−OH)-$RuH(PPh_3)_2(CO)$][Cl] (**2a**) (Scheme 2). The ^{1}H NMR spectrum of **2a** in CD_3OD exhibits several groups of signals between 8.68 and 6.30 ppm for the pyridyl and PPh_3 groups (39H), one singlet at 3.91 ppm for the $-CH_2-$ group (2H), and one triplet at −11.90 ppm for Ru−H (1H). The ^{31}P NMR shows one singlet at 45.62 ppm. The IR spectrum displays one absorption peak at 1958 cm^{-1} (in DCM) for the terminal CO. These results indicate there are two *trans*-PPh_3, one CO, one hydride, and two pyridyl rings of ligand **L₁** coordinating with Ru. However, it was still difficult to confirm its exact coordination geometry without its single-crystal structure.

Scheme 2. Synthesis of Complexes 2a−c

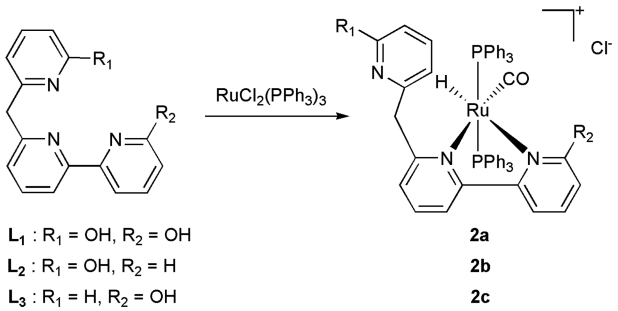

Ligand precursors **L₂** and **L₃** were then treated with $RuHCl(PPh_3)_3(CO)$, and complexes [(HO-C_5H_3N-CH_2-C_5H_3N-C_5H_4N)$RuH(PPh_3)_2(CO)$][Cl] (**2b**) and [(C_5H_4N-CH_2-C_5H_3N-C_5H_3N-OH)$RuH(PPh_3)_2(CO)$][Cl] (**2c**) were afforded, respectively (Scheme 2).

The ^{1}H NMR spectrum of **2b** in CD_3OD shows a triplet for the Ru−H group at −10.90 ppm. The ^{31}P NMR spectrum shows one singlet for the two PPh_3 groups at 45.7 ppm. The IR spectrum exhibits a strong CO absorption at 1947 cm^{-1} (in DCM). Complex **2c** displays similar NMR and IR spectra, indicating their analogous structures.

The structure of **2c** was further characterized by X-ray crystallography (Figure 2). The Ru ion is coordinated in an octahedral geometry. The ligand **L₃** coordinates with the Ru atom via its bipyridyl N atoms. The CO ligand is trans to the middle pyridyl ring, and the hydride is trans to the pyridinol group. The two PPh_3 groups are in trans positions.

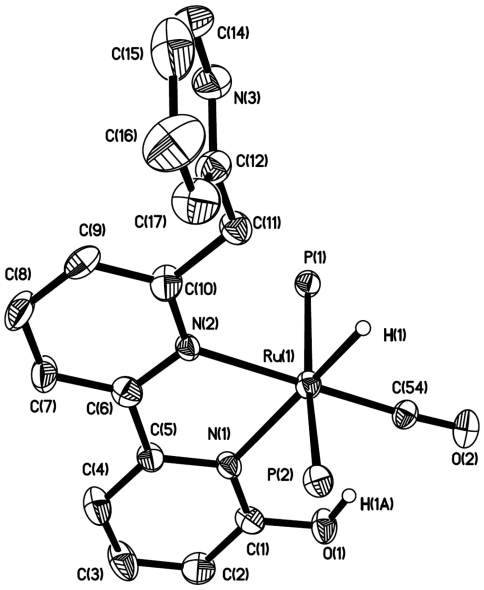

Figure 2. Solid-state structure of complex **2c**. The thermal ellipsoids are displayed at 30% probability. Hydrogen atoms (except Ru−H and −OH), phenyl rings on PPh_3 ligands, and the Cl^- anion have been omitted for clarity. Selected bond distances (Å): Ru(1)−N(1), 2.204(6); Ru(1)−N(2), 2.178(6); Ru(1)−P(1), 2.373(2); Ru(1)−P(2), 2.379(2); Ru(1)−C(54), 1.816(8); Ru(1)−H(1), 1.657; C(5)−N(1), 1.367(9); N(1)−C(1), 1.325(9); O(1)−C(1), 1.338(9); C(1)−C(2), 1.382(10); O(1)−H(1A), 0.820.

Complex **2a** was then treated with 2 equiv of *t*-BuOK, and the product [(O-C_5H_3N-CH_2-C_5H_3N-C_5H_3N-OH)RuH-(PPh_3)(CO)] (**3a**) was obtained in 98% yield (Scheme 3). Different from complex **2a**, the ^{1}H NMR spectrum of **3a** shows two doublets at 5.19 and 4.15 ppm for the $-CH_2$ group, which means that the third pyridyl ring also coordinates with Ru. The doublet at −12.68 ppm for the Ru−H indicates only one PPh_3 left. The IR peak at 1935 cm^{-1} corresponds to a terminal CO. Its red-shifted phenomenon in comparison to complex **2a** is ascribed to enhanced electron density at the metal center upon ligand deprotonation, leading to greater donation into the CO π^* orbitals ($\Delta\nu$ = −23 cm^{-1}).[18a] The solid-state structure reveals its exact geometry (Figure 3). The O(2)−C(16)

DOI: 10.1021/acs.organomet.8b00432
Organometallics XXXX, XXX, XXX−XXX

Scheme 3. Synthesis of Complexes 3a,b

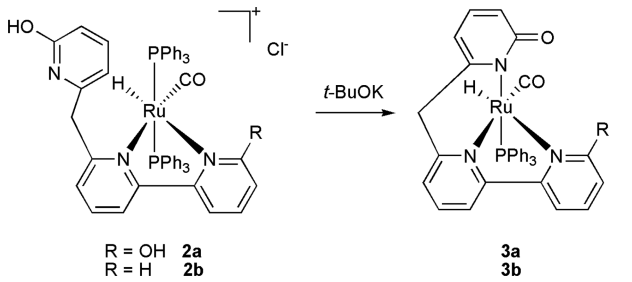

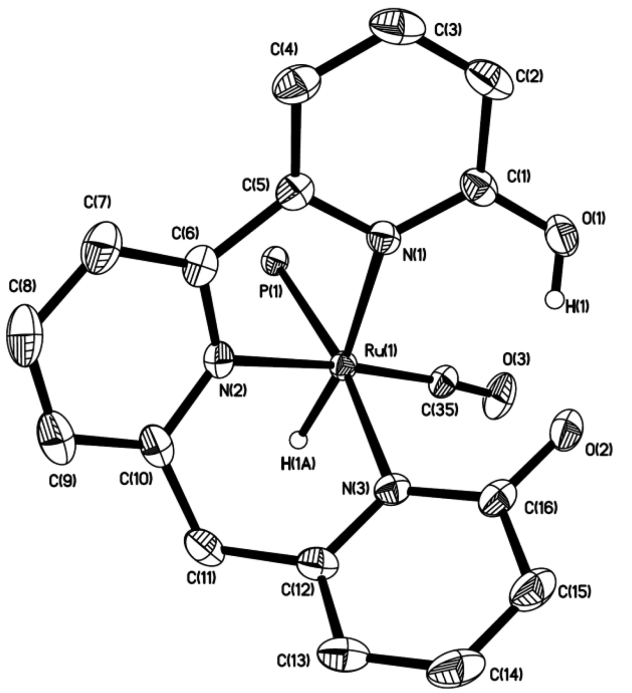

Figure 3. Solid-state structure of complex **3a**. The thermal ellipsoids are displayed at 30% probability. Hydrogen atoms (except Ru−H and −OH) and phenyl rings on PPh_3 ligand have been omitted for clarity. Selected bond distances (Å): Ru(1)−N(1), 2.231(2); Ru(1)−N(2), 2.128(2); Ru(1)−N(3), 2.142(2); Ru(1)−P(1), 2.3051(7); Ru(1)−C(35), 1.824(3); Ru(1)-H(1A), 1.458; C(15)−H(16), 1.419(5); O(2)−C(16), 1.291(4); N(3)−C(16), 1.361(4); N(3)−C(12), 1.361(4); C(12)−C(11), 1.521(5); C(10)−C(11), 1.500(5); N(2)−C(10), 1.349(4); N(2)−C(6), 1.348(4); C(5)−C(6), 1.477(4); N(1)−C(5), 1.361(4); N(1)−C(1), 1.343(4); O(1)−C(1), 1.309(4); O(1)−H(1), 0.820; C(2)−C(1), 1.410(5).

distance (1.291(4) Å) is similar to those of a pyridinol diruthenium complex supported by deprotonated 6,6′-dihydroxyterpyridine developed by Szymczak's group, suggesting a C═O bond.[18a] The C−O single distance (O(1)−C(1), 1.309(4) Å) is also comparable to those of Szymczak's ruthenium complexes.[18a] This means that the −OH group of $PyCH_2PyOH$ is more acidic than that of PyPyOH, or else H(1) would transfer to the pyridinol moiety. The results suggested complex **3a** was formed by the selective deprotonation of the −OH group in the uncoordinated 2-hydroxypyridyl ring of complex **2a**, followed by the substitution of one PPh_3. The three pyridyl rings are mutually cis and are not in the same plane. Even though excess *t*-BuOK was used, the other −OH group and the $-CH_2-$ group were unreactive.

Complex **2b** exhibited reactivity similar to that of **2a** with *t*-BuOK, and $[(O\text{-}C_5H_3N\text{-}CH_2\text{-}C_5H_3N\text{-}C_5H_4N)RuH(PPh_3)(CO)]$ (**3b**) was afforded within 10 min (Scheme 3). Complex **3b** was identified by ^1H and ^{31}P NMR, IR, elemental analysis, and X-ray crystallography (Figure 4).

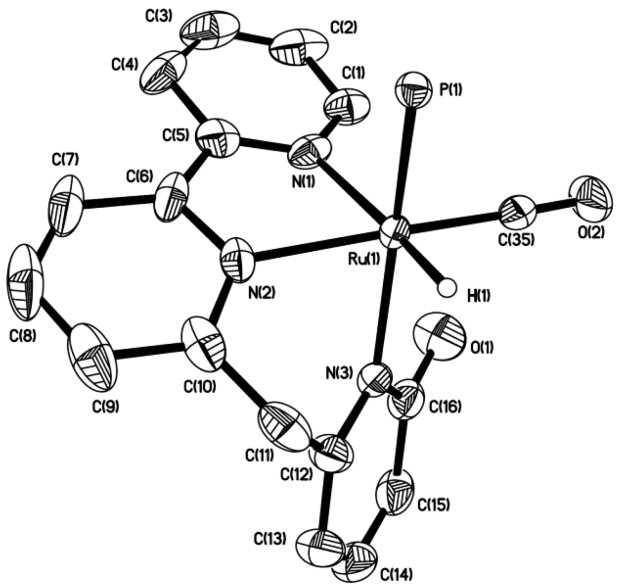

Figure 4. Solid-state structure of complex **3b**. The thermal ellipsoids are displayed at 30% probability. Hydrogen atoms (except Ru−H) and phenyl rings on the PPh_3 ligand have been omitted for clarity. Selected bond distances (Å): Ru(1)−N(1), 2.186(3); Ru(1)−N(2), 2.125(3); Ru(1)−N(3), 2.156(3); Ru(1)−P(1), 2.2804(9); Ru(1)−C(35), 1.823(4); Ru(1)-H(1A), 1.580; C(15)−H(16), 1.431(7); O(1)−C(16), 1.251(6); N(3)−C(16), 1.371(5); N(3)−C(12), 1.354(5); C(12)−C(11), 1.525(7); C(10)−C(11), 1.479(7); N(2)−C(10), 1.332(6); N(2)−C(6), 1.379(6); C(5)−C(6), 1.438(7); N(1)−C(5), 1.301(6); N(1)−C(1), 1.354(6); C(2)−C(1), 1.373(7).

The reactivity of complex **2c** with *t*-BuOK was slightly different from that of **2a**,**b**, and the two products $[(C_5H_4N\text{-}CH_2\text{-}C_5H_3N\text{-}C_5H_3N\text{-}O)RuH(PPh_3)_2(CO)]$ (**3c**) and $[(C_5H_4N\text{-}CH_2\text{-}C_5H_3N\text{-}C_5H_3N\text{-}O)RuH(PPh_3)(CO)]$ (**3d**) were obtained in 56% and 11% yields, respectively, after reflux in isopropyl alcohol for 24 h. Complex **3c** could also be transformed to **3d** with 10% yield without any other additives, also after reflux in isopropyl alcohol for 24 h. However, in the presence of 10 equiv of PPh_3, complex **3d** was completely converted back to **3c** (Scheme 4). It should be noted that complexes **2c** and **3c** have the same polarity, and so they might be mistakenly regarded as the same compound. Significant differences are observed in their ^1H NMR, ^{31}P NMR, and IR spectra. The ^1H NMR spectrum of complex **3c** in CD_3OD

Scheme 4. Synthesis and Relationship of Complexes 3c,d

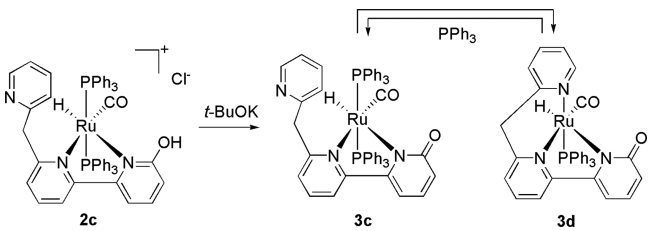

DOI: 10.1021/acs.organomet.8b00432
Organometallics XXXX, XXX, XXX−XXX

Table 1. β-Alkylation of 1-Phenylethanol with Benzyl Alcohol Using Ru Complexes 2a−c and 3a−d[a]

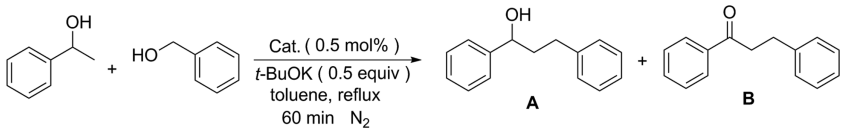

entry	catalyst	conv (%)[b]	A:B ratio[c]
1	**2a**	51	98:2
2	**2b**	70	98:2
3	**2c**	94	95:5
4	**3a**	26	88:12
5	**3b**	36	90:10
6	**3c**	94	96:4
7	**3d**	70	86:14

[a]Reaction conditions: catalyst (0.5 mol %), 1-phenylethanol (2.0 mmol), benzyl alcohol (2.0 mmol), and *t*-BuOK (1 mmol) at reflux in toluene for 60 min under an N_2 atmosphere. [b]Determined by GC analysis on the basis of secondary alcohol. [c]Determined by GC analysis.

Table 2. β-Alkylation of 1-Phenylethanol with Benzyl Alcohol in the Presence of Different Bases[a]

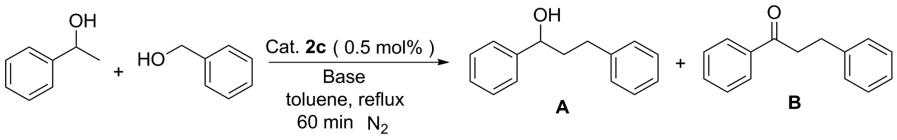

entry	base (amt (equiv))	conv (%)[b]
1	Na_2CO_3 (0.5)	2
2	K_2CO_3 (0.5)	4
3	Cs_2CO_3 (0.5)	5
4	KOH (0.5)	85
5	NaOH (0.5)	91
6	*t*-BuOK (0.5)	94
7	*t*-BuOK (0.4)	88
8	*t*-BuOK (0.3)	78
9	*t*-BuOK (0.2)	56
10	*t*-BuOK (0.1)	44
11[c]	*t*-BuOK (0.5)	94
12	no base	0
13[d]	*t*-BuOK (0.5)	0
14[e]	*t*-BuOK (0.5)	52

[a]Reaction conditions unless specified otherwise: catalyst **2c** (0.5 mol %), 1-phenylethanol (2.0 mmol), benzyl alcohol (2.0 mmol), and base at reflux in toluene for 60 min. [b]Determined by GC analysis on the basis of secondary alcohol. [c]The reaction was carried out in an air atmosphere. [d]No catalyst. [e]The reaction was carried out at 90 °C.

shows no signal between 8.00 and 7.70 ppm, while that of **2c** shows a doublet at 7.88 ppm. Their singlet of the $-CH_2-$ group and the triplet of the Ru−H group are also slightly different (4.24 and −11.26 ppm for **3c**; 4.16 and −11.39 ppm for **2c**). The ^{31}P NMR spectrum of complex **3c** shows one singlet for the two PPh_3 groups at 46.2 ppm in $CDCl_3$, comparable to that of **2c** (47.6 ppm). The CO absorptions of complexes **3c** and **2c** exhibit a $\Delta\nu$ value of 9 cm^{-1} (1945 cm^{-1} for **3c** and 1954 cm^{-1} for **2c**). Complex **3d** was also identified by ^1H and ^{31}P NMR, IR, and elemental analysis, and the spectroscopic analysis indicates that it displays a structure similar to that of **3a**,**b**.

We further calculated the relative free energies of **3c**,**d** using the DFT method and found that **3d** was higher than **3c** by 7.4 kcal/mol. This result explains the low yield of **3d**, and it is consistent with the observed conversion of **3d** to **3c** in the presence of PPh_3.

No bidentate product similar to **3c** was detected when complex **2a** was treated with *t*-BuOK, indicating that the nucleophilicity of the deprotonated uncoordinated 2-hydroxypyridyl in **2a** is stronger than that of pyridyl in **2c**, and as long as the deprotonated intermediate formed, the pyridinol group attacked the ruthenium center, accompanied by the loss of one PPh_3. The results further support that it was the −OH group of the $PyCH_2PyOH$ moiety that was deprotonated during the reaction.

β-Alkylation of Secondary Alcohols with Primary Alcohols. Initially, the coupling of 1-phenylethanol and benzyl alcohol was selected as a model reaction to test the catalytic activity of complexes **2a−c** and **3a−d**. The reactions were conducted in toluene at 110 °C for 60 min. Ruthenium complexes (0.5 mol %) were used as the precatalysts and *t*-BuOK (0.5 equiv) as the base under an N_2 atmosphere, and the results are shown in Table 1. It can be seen that complexes **2c** and **3c** show the highest catalytic activity, giving 94% conversion within 60 min in both cases (entries 3 and 6). The tridentate complexes **3a**,**b**,**d** are not as active as the bidentate complexes **2a−c**, indicating that they are not the reaction intermediates of those bidentate complexes. The catalytic

DOI: 10.1021/acs.organomet.8b00432
Organometallics XXXX, XXX, XXX−XXX

Table 3. β-Alkylation of 1-Phenylethanol and Its Derivatives with a Variety of Primary Alcohols[a]

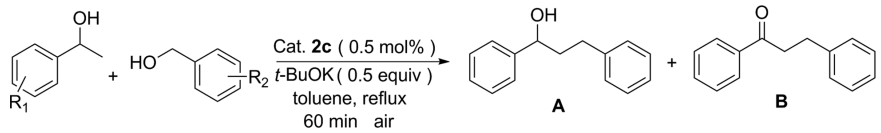

Entry	Primary	Secondary	Product	Conv.[%][b]	A/B Ratio[b]
1	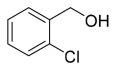		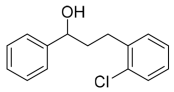	89	86:14
2	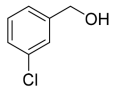		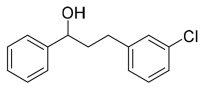	93	98:2
3	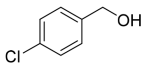		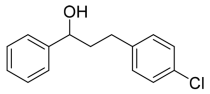	94	100:0
4	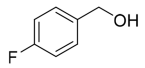		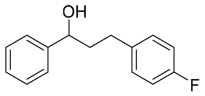	97	100:0
5	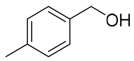		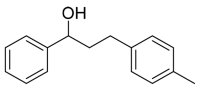	95	100:0
6	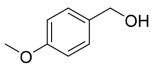		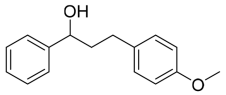	93	100:0
7	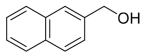		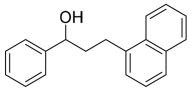	95	100:0
8	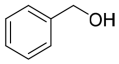	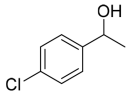	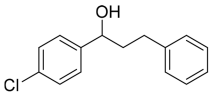	90	91:9
9[c]	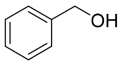	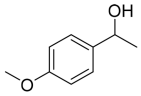	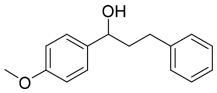	83	75:25

[a]Reaction conditions unless specified otherwise: catalyst **2c** (0.5 mol %), 1-phenylethanol (2.0 mmol), benzyl alcohol (2.0 mmol), and *t*-BuOK (1 mmol) at reflux in toluene for 60 min in an air atmosphere. [b]Determined by GC analysis on the basis of secondary alcohol. [c]2 h reflux.

activities of complexes **2c** and **3c** are similar, suggesting **3c** is the catalytic intermediate of **2c**.

Subsequently, to optimize the reaction conditions for β-alkylation of 1-phenylethanol with benzyl alcohol catalyzed by **2c**, other bases were tested, and the results are given in Table 2. Weak bases such as Na_2CO_3, K_2CO_3, and Cs_2CO_3 revealed low conversion in the reaction (entries 1−3). When strong bases such as KOH, *t*-BuOK, and NaOH were chosen, the conversion rate was significantly increased (entries 4−6). For example, a 94% conversion within 60 min was achieved when *t*-BuOK was used. Next, to optimize the base quantity required, different amounts of *t*-BuOK were tested, and 0.5 equiv was the best (entries 6−10). Unexpectedly, when the reaction was carried out in an air atmosphere, the conversion rate did not decrease (entry 11). This was encouraging because such reactions usually require an N_2 atmosphere.[17b,c,23,24] Without a catalyst or base, the reaction failed to take place (entries 12 and 13). When the reaction was carried at 90 °C,

DOI: 10.1021/acs.organomet.8b00432
Organometallics XXXX, XXX, XXX−XXX

Table 4. β-Alkylation of 1-Phenylethanol with Benzyl Alcohol Using Ru Complexes 3c−e for Different Times[a]

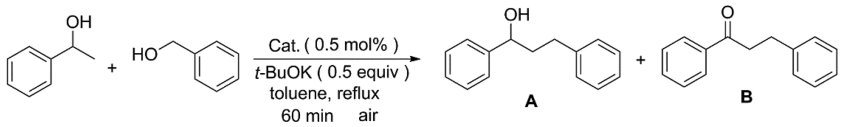

entry	catalyst	time (min)	conv (%)[b]
1	**3c**	5	13
2	**3d**	5	14
3	**3c**	10	28
4	**3d**	10	25
5	**3c**	20	58
6	**3d**	20	39
7	**3c**	30	75
8	**3d**	30	59
9	**3c**	60	94
10	**3d**	60	70
11[c]	**3e**	60	60

[a]Reaction conditions unless specified otherwise: catalyst (0.5 mol %), 1-phenylethanol (2.0 mmol), benzyl alcohol (2.0 mmol), and *t*-BuOK (1 mmol) at reflux in toluene for 60 min in an air atmosphere. [b]Determined by GC analysis on the basis of secondary alcohol. [c]Catalyst (0.25 mol %).

the conversion was decreased to 52% within 60 min (entry 14).

On the basis of the above results, the optimized reaction conditions were established (entry 3 in Table 1 and entry 11 in Table 2). β-alkylation of 1-phenylethanol and its derivatives with a variety of primary alcohols was performed. As shown in Table 3, most substrates exhibit excellent conversion and selectivity except for entries 1 and 9. From entries 1−3, it can be observed that the chloro-substituted benzyl alcohols at a meta or para position convert to the desired secondary alcohols with 1-phenylethanol in higher conversion and selectivity in comparsion to that at an ortho position, probably due to a steric hindrance effect. In addition, no obvious substituent effect is observed when either an electron-withdrawing group or an electron-donating group is introduced to the para position of benzyl alcohol (entries 3−6). Furthermore, naphthalen-1-ylmethanol also has a good conversion (95%) and selectivity (100:0) (entry 7). On the other hand, an electron-withdrawing group at the para position of 1-phenylethanol does not obviously influence the reaction, while an electron-donating group decreases the activity and selectivity dramatically (entries 8 and 9).

As shown in Table 1, complex **3d** is not as active as **3c** in 60 min. However, at shorter reaction times (5 and 10 min), their catalytic activities are similar (Table 4, entries 1−4). We hypothesized this phenomenon might be due to the relative instability of **3d**.

To test our hypothesis, complex **3d** was then heated in refluxing toluene, and the diruthenium complex $[(C_5H_4N\text{-}CH\text{-}C_5H_3N\text{-}C_5H_3N\text{-}O)Ru(PPh_3)(CO)]_2$ (**3e**) was obtained (Scheme 5). Different from complex **3d**, the characteristic peak for Ru−H disappeares in the ^{1}H NMR spectrum of **3e**. The IR absorption at 1939 cm^{-1} corresponds to the terminal CO groups. The X-ray crystallographic structure shows that **3e** is a diruthenium complex with C_i symmetry, and the Ru(1)−C(11A) bond is formed via C−H activation of the $-CH_2-$ group (Figure 5). As expected, complex **3e** is not as active as **3c**,**d** with the same amount of Ru atoms (Table 4, entry 11), which explains why **3c** is more active than **3d** over a longer period of time (Table 4, entries 5−10).

Scheme 5. Synthesis of 3e

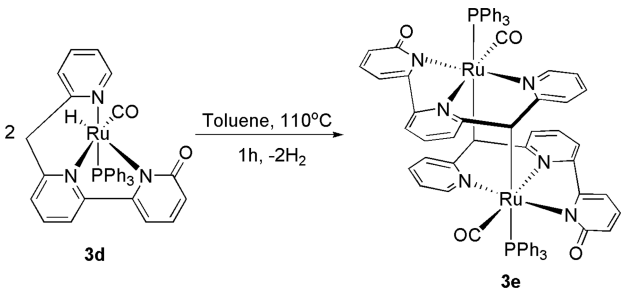

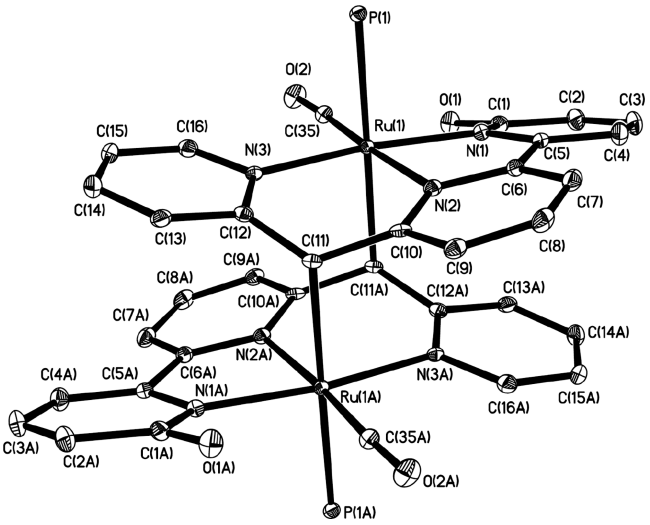

Figure 5. Solid-state structure of complex **3e**. The thermal ellipsoids are displayed at 30% probability. Hydrogen atoms and phenyl rings on the PPh_3 ligand have been omitted for clarity. Selected bond distances (Å): Ru(1)−N(1), 2.086(3); Ru(1)−N(2), 2.104(3); Ru(1)−N(3), 2.122(3); Ru(1)−P(1), 2.3666(9); Ru(1)−C(35), 1.845(4); Ru(1)−C(11), 2.296(3); C(1)−C(2), 1.428(5); O(1)−C(1), 1.257(5); N(1)−C(1), 1.392(4); N(1)−C(5), 1.367(5); C(5)−C(6), 1.477(5); C(6)−N(2), 1.365(4); N(2)−C(10), 1.349(4); C(10)−C(11), 1.463(5); C(11)−C(12), 1.466(5); N(3)−C(12), 1.364(4).

Reaction Mechanism. On the basis of relevant literature, a plausible mechanism for this tandem β-alkylation of secondary

DOI: 10.1021/acs.organomet.8b00432
Organometallics XXXX, XXX, XXX−XXX

Scheme 6. Proposed Reaction Mechanism

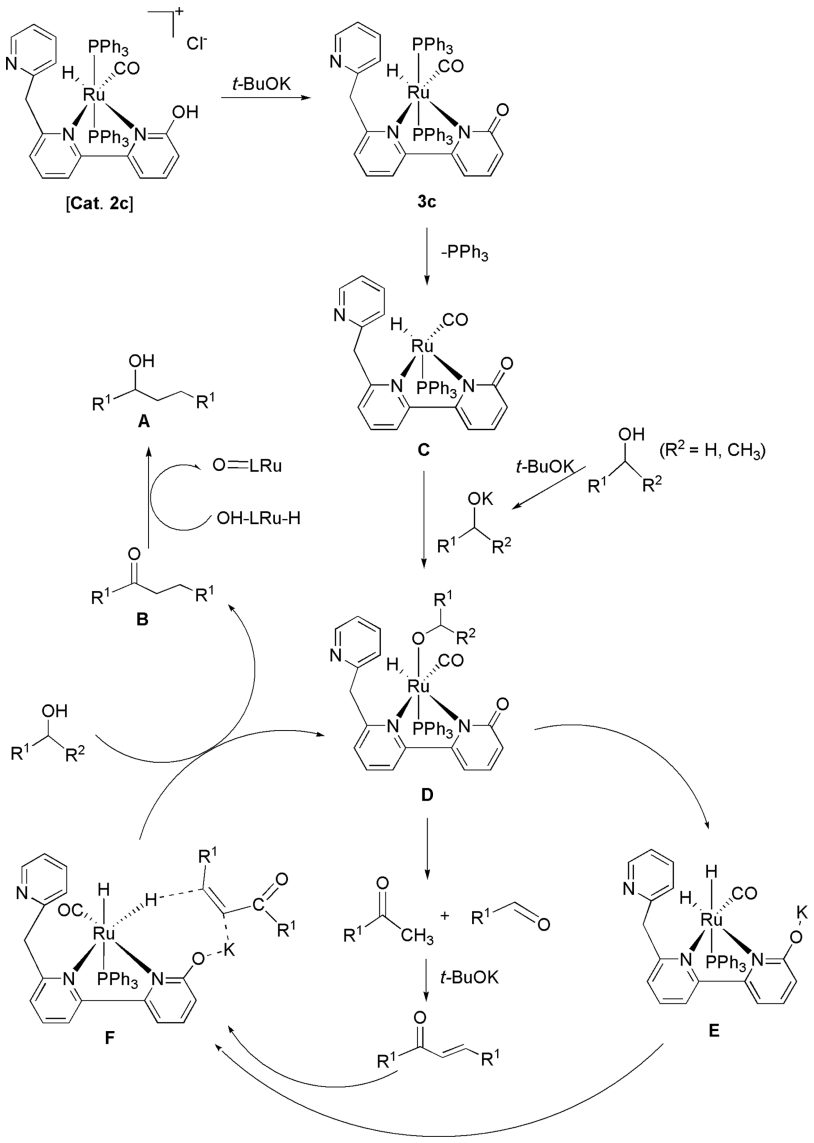

alcohols with primary alcohols catalyzed by **2c** is shown in Scheme 6.[17b,c] In the presence of *t*-BuOK, precatalyst **2c** first transforms to **3c** with a 2-pyridinol ligand via dearomatization by extrusion of one molecule of HCl. Then, **3c** loses one molecule of PPh_3 to form the active intermediate **C** with an open site. **C** further reacts with potassium alkoxide to generate the alkoxy ruthenium species **D**. A similar K^+-bound alkoxide intermediate has been confirmed in Szymczak's system.[18a] **D** undergoes *β*-H elimination by releasing one molecule of carbonyl compounds to afford the dihydride Ru(II) species **E**. Next, a base-catalyzed cross-aldol condensation between the ketones and aldehydes affords *α*,*β*-unsaturated ketones. Finally, the Ru hydride and the K^+ in **F** cooperate to promote the hydrogenation of a C═C bond of the *α*,*β*-unsaturated ketones, resulting in the regeneration of **C** and the formation of ketone **B**. **B** could be further converted to **A** following a similar cooperative process.

In order to further investigate whether dissociation of PPh_3 is involved in the catalytic cycle, the *β*-alkylation of 1-phenylethanol with benzyl alcohol was performed in the presence of excess PPh_3 (2−8 equiv) (Figure 6).[17b,18e] It was

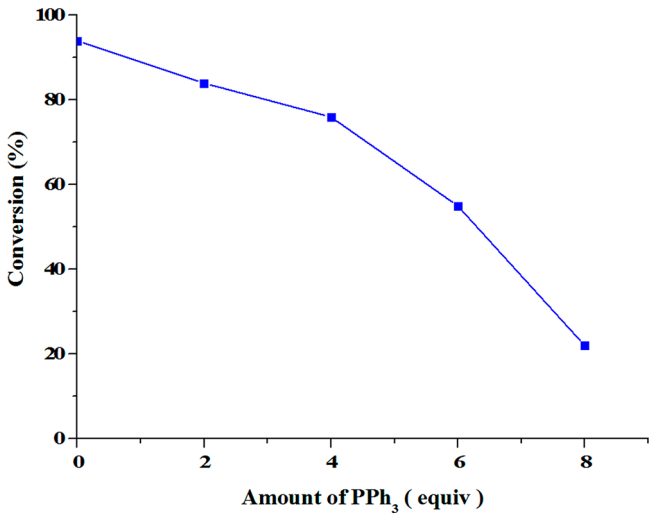

Figure 6. Effect of externally added PPh_3 on catalyst **2c** in *β*-alkylation of 1-phenylethanol with benzyl alcohol.

DOI: 10.1021/acs.organomet.8b00432
Organometallics XXXX, XXX, XXX−XXX

observed that the conversion of 1-phenylethanol continuously decreased with increasing amounts of PPh_3. The above experimental results demonstrated that the elimination of PPh_3 played a vital role in the catalytic cycle. However, as intermediates **C**−**F** have not been isolated, a detailed mechanistic analysis requires further investigation.

■ CONCLUSIONS

In summary, the three bidentate ruthenium hydride complexes **2a**−**c** with several proton-responsive sites supported by unsymmetrical NNN ligands were synthesized. Reactions of **2a**,**b** with *t*-BuOK gave tridentate products **3a**,**b**, respectively, via selective deprotonation of the −OH group of the $PyCH_2PyOH$ moiety. The results indicate the −OH group of the $PyCH_2PyOH$ moiety is more acidic than that of PyPyOH and the $-CH_2-$ group. The reactivity with *t*-BuOK of **2c** was different from that of **2a**,**b**. In addition to the tridentate product **3d**, the bidentate product **3c** was also obtained. It is more difficult for the pyridyl group to replace PPh_3 than the deprotonated pyridinol group, because of their nucleophilic difference. Although the $-CH_2-$ group in **3d** is not reactive with *t*-BuOK, it can be activated by the other molecule of **3d** to form **3e** with H_2 release. The aforementioned eight complexes were tested as catalysts for *β*-alkylation of secondary alcohols with primary alcohols, and the bidentate complexes **2c** and **3c** showed the highest activity. The conversion reached 94% in 60 min with 0.5 mol % of catalyst in both cases, when 1-phenylethanol and benzyl alcohol were used as substrates. As an unexpected benefit, these reactions were not compromised in air. The tridentate complexes **3a**,**b**,**d** are less active than the corresponding bidentate complexes, indicating they are not the intermediates of **2a**−**c**, and the lower efficiency of **3d** in comparison to **3c** is due to its dimerization behavior to form **3e**. However, **3c** can be regarded as the intermediate of **2c**, confirming that the catalytic transformation undergoes an aromatization−dearomatization process. The results in this paper are important for developing more efficient bifunctional catalysts for *β*-alkylation of secondary alcohols with primary alcohols.

■ EXPERIMENTAL SECTION

General Considerations. All manipulations were carried out under an inert nitrogen atmosphere using a Schlenk line. Solvents were distilled from the appropriate drying agents under N_2 before use. All reagents were purchased from commercial sources. Liquid compounds were degassed by standard freeze−pump−thaw procedures prior to use. $RuHCl(PPh_3)_3(CO)$[25] and $\mathbf{L_1}$−$\mathbf{L_3}$[22a] were prepared as previously described, respectively. The ^1H and ^{31}P NMR spectra were recorded on a Bruker Avance 400 spectrometer. The ^1H NMR chemical shifts were referenced to residual solvent as determined relative to Me_4Si (*δ* 0 ppm). The $^{31}P\{^1H\}$ chemical shifts were reported in ppm relative to external 85% H_3PO_4. Elemental analyses were performed on a PerkinElmer 240C analyzer. X-ray diffraction studies were carried out in a SuperNova X-ray single-crystal diffractometer. Data collections were performed using four-circle kappa diffractometers equipped with CCD detectors. Data were reduced and then corrected for absorption. Solution, refinement, and geometrical calculations for all crystal structures were performed by SHELXTL.

General Procedure for *β*-Alkylation of Secondary Alcohols with Primary Alcohol. The catalytic *β*-alkylation of secondary alcohol reaction was carried out in a flask in air. Initially catalyst **2c** (0.5 mol %) and *t*-BuOK (0.5 equiv) were taken as solids and then in air a secondary alcohol (1 equiv), primary alcohol (1 equiv), and toluene (3 mL) were added; the resulting mixture was heated at 110 °C (oil bath temperature) for 60 min. After the mixture was cooled to room temperature, the toluene was evaporated under reduced pressure and the resulting mixture was purified by silica gel column chromatography using ethyl acetate and hexane as eluent to afford the desired product.

*Synthesis of **2a**.* A solution of $\mathbf{L_1}$ (0.18 g, 0.63 mmol) and $RuHCl(PPh_3)_3(CO)$ (0.60 g, 0.63 mmol) was heated in refluxing methanol (200 mL) for 24 h. The mixture was cooled to room temperature, and the organic phase was evaporated under vacuum. The crude product was recrystallized with dichloromethane/ether to give **2a** as a yellow powder (0.47 g, 78%). Anal. Calcd for $C_{53}H_{44}ClN_3O_3P_2Ru$: C, 65.67; H, 4.57; N, 4.33. Found: C, 65.96; H, 4.63; N, 4.26. ^1H NMR (400 MHz, CD_3OD, ppm): 8.68 (d, *J* = 5.2 Hz, 1H), 8.30 (d, *J* = 8.0 Hz, 1H), 8.23 (d, *J* = 8.0 Hz, 1H), 7.93−7.82 (m, 3H), 7.43−7.13 (m, 31H), 6.73 (d, *J* = 8.0 Hz, 1H), 6.30 (d, *J* = 9.2 Hz, 1H), 3.91 (s, 2H), −11.90 (t, *J* = 18.4 Hz, 1H). ^{31}P NMR (162 MHz, CD_3OD, ppm): 45.6. IR (ν_{CO}, in DCM, cm^{-1}): 1958 (s).

*Synthesis of **2b**.* A solution of $\mathbf{L_2}$ (0.17 g, 0.63 mmol) and $RuHCl(PPh_3)_3(CO)$ (0.60 g, 0.63 mmol) was heated in refluxing methanol (200 mL) for 24 h. The mixture was cooled to room temperature, and the organic phase was evaporated under vacuum. The crude product was recrystallized with dichloromethane/ether to give **2b** as a yellow powder (0.38 g, 63%). Anal. Calcd for $C_{53}H_{44}ClN_3O_2P_2Ru$: C, 66.77; H, 4.65; N, 4.41. Found: C, 66.65; H, 4.50; N, 4.46. ^1H NMR (400 MHz, CD_3OD, ppm): 8.69 (d, *J* = 3.2 Hz, 1H), 8.30 (d, *J* = 5.2 Hz, 1H), 8.23 (d, *J* = 5.6 Hz, 1H), 7.91 (t, *J* = 5.6 Hz, 1H), 7.84 (t, *J* = 5.4 Hz, 1H), 7.43−7.21 (m, 31H), 7.19−7.14 (m, 2H), 6.73 (d, *J* = 5.2 Hz, 1H), 6.30 (d, *J* = 6.0 Hz, 1H), 3.91 (s, 2H), −10.90 (t, *J* = 12.0 Hz, 1H). ^{31}P NMR (162 MHz, CD_3OD, ppm): 45.7. IR (ν_{CO}, in DCM, cm^{-1}): 1947 (s).

*Synthesis of **2c**.* A solution of $\mathbf{L_3}$ (0.17 g, 0.63 mmol) and $RuHCl(PPh_3)_3(CO)$ (0.60 g, 0.63 mmol) was heated in refluxing methanol (200 mL) for 24 h. The mixture was cooled to room temperature, and the organic phase was evaporated under vacuum. The crude product was recrystallized with acetone to give **2c** as a yellow powder (0.38 g, 63%). A crystal suitable for a single-crystal X-ray diffraction experiment was grown by vapor diffusion of *n*-hexane into a dichloromethane solution of **2c** at room temperature. Anal. Calcd for $C_{53}H_{44}ClN_3O_2P_2Ru$: C, 66.77; H, 4.65; N, 4.41. Found: C, 66.96; H, 4.76; N, 4.40. ^1H NMR (400 MHz, CD_3OD, ppm): 8.34 (d, *J* = 5.6 Hz, 1H), 7.88 (d, *J* = 8.0 Hz, 1H), 7.65 (t, *J* = 7.6 Hz, 1H), 7.59 (m, 2H), 7.48 (m, 1H), 7.40−7.18 (m, 30H), 7.17−7.13 (m, 1H), 6.73 (d, *J* = 8.0 Hz, 1H), 6.37 (d, *J* = 7.6 Hz, 1H), 6.18 (d, *J* = 7.6 Hz, 1H), 4.16 (s, 2H), −11.39 (t, *J* = 19.2 Hz, 1H). ^{31}P NMR (162 MHz, CD_3OD, ppm): 47.6. IR (ν_{CO}, in DCM, cm^{-1}): 1954 (s).

*Synthesis of **3a**.* A solution of **2a** (1.0 g, 1.0 mmol) and *t*-BuOK (0.22 g, 2.0 mmol) was heated in refluxing isopropyl alcohol (300 mL) for 24 h. The mixture was cooled to room temperature, and the organic phase was evaporated under vacuum. The crude product was recrystallized with acetone to give **3a** as an orange-red powder (0.64 g, 98%). A crystal suitable for a single-crystal X-ray diffraction experiment was grown by vapor diffusion of *n*-hexane into a dichloromethane solution of **3a** at room temperature. Anal. Calcd for $C_{35}H_{28}N_3O_3PRu$: C, 62.68; H, 4.21; N, 6.27. Found: C, 62.45; H, 4.40; N, 6.12. ^1H NMR (400 MHz, $CDCl_3$, ppm): 16.19 (s, 1H), 7.54 (br s, 1H), 7.33−7.06 (m, 19H), 6.84 (br s, 1H), 6.72 (d, *J* = 7.6 Hz, 1H), 6.56 (d, *J* = 7.6 Hz, 1H), 6.45 (br s, 1H), 5.19 (d, *J* = 13.6 Hz, 1H), 4.15 (d, *J* = 13.6 Hz, 1H), −12.68 (d, *J* = 28.8 Hz, 1H). ^{31}P NMR (162 MHz, $CDCl_3$, ppm): 59.0. IR (ν_{CO}, in DCM, cm^{-1}): 1935 (s).

*Synthesis of **3b**.* A solution of **2b** (1.0 g, 1.0 mmol) and *t*-BuOK (0.22 g, 2.0 mmol) was heated in refluxing isopropyl alcohol (300 mL) for 10 min. The mixture was cooled to room temperature, and the organic phase was evaporated under vacuum. The crude product was recrystallized with acetone to give **3b** as an orange-red powder (0.60 g, 92%). A crystal suitable for a single-crystal X-ray diffraction experiment was grown by vapor diffusion of *n*-hexane into a dichloromethane solution of **3b** at room temperature. Anal. Calcd for $C_{35}H_{28}N_3O_2PRu$: C, 64.21; H, 4.31; N, 6.42. Found: C, 64.12; H, 4.45; N, 6.42. ^1H NMR (400 MHz, $CDCl_3$, ppm): 9.49 (br s, 1H),

DOI: 10.1021/acs.organomet.8b00432
Organometallics XXXX, XXX, XXX−XXX

7.72−6.99 (m, 23H), 6.22−6.08 (m, 1H), 5.11 (d, J = 13.6 Hz, 1H), 4.13 (d, J = 13.6 Hz, 1H), −12.01 (d, J = 29.0 Hz, 1H). ^{31}P NMR (162 MHz, $CDCl_3$, ppm): 59.1. IR (ν_{CO}, in DCM, cm^{-1}): 1935 (s).

*Synthesis of **3c,d**.* A solution of **2c** (1.0 g, 1.0 mmol) and *t*-BuOK (0.22 g, 2.0 mmol) was heated in refluxing isopropyl alcohol (300 mL) for 24 h. The mixture was cooled to room temperature, and the organic phase was evaporated under vacuum to provide a mixture of **3c** and **3d**. The mixture was purified by column chromatography on silica gel (eluent: ethyl acetate/methanol, 5/1 v/v) to give **3c** (0.51 g, 56%) as a yellow powder and **3d** (0.07 g, 11%) as a brown powder. **3c** could also transform to **3d** in 10% yield without any other additives in refluxing isopropyl alcohol for 24 h. When **3d** was added to 10 equiv of PPh_3 in refluxing isopropyl alcohol for 24 h, **3d** transformed completely into **3c**. Data for **3c** are as follows. Anal. Calcd for $C_{53}H_{43}N_3O_2P_2Ru$: C, 69.42; H, 4.73; N, 4.58. Found: C, 69.35; H, 4.62; N, 4.52. ^{1}H NMR (400 MHz, CD_3OD, ppm): 8.34 (d, J = 4.8 Hz, 1H), 7.62 (d, J = 8.0 Hz, 1H), 7.51−7.14 (m, 34H), 6.99 (d, J = 7.2 Hz, 1H), 6.56 (d, J = 8.4 Hz, 1H), 6.33 (d, J = 7.6 Hz, 1H), 6.08 (d, J = 8.0 Hz, 1H), 4.24 (s, 2H), −11.26 (t, J = 19.2 Hz, 1H). ^{31}P NMR (162 MHz, $CDCl_3$, ppm): 46.2. IR (ν_{CO}, in DCM, cm^{-1}): 1945 (s). Data for **3d** are as follows. Anal. Calcd for $C_{35}H_{28}N_3O_2PRu$: C, 64.21; H, 4.31; N, 6.42. Found: C, 64.13; H, 4.22; N, 6.35. ^{1}H NMR (400 MHz, CD_3OD, ppm): 9.53 (d, J = 5.2 Hz, 1H), 7.75−7.66 (m, 3H), 7.51 (d, J = 7.6 Hz, 1H), 7.45 (d, J = 8.0 Hz, 1H), 7.36−7.13 (m, 17H), 6.84 (d, J = 7.2 Hz, 1H), 6.36 (d, J = 8.4 Hz, 1H), 5.11 (d, J = 13.6 Hz, 1H), 4.48 (d, J = 14.0 Hz, 1H), −12.16 (d, J = 28.8 Hz, 1H). ^{31}P NMR (162 MHz, CD_3OD, ppm): 60.7. IR (ν_{CO}, in DCM, cm^{-1}): 1938 (s).

*Synthesis of **3e**.* A solution of **3d** (0.1 g, 0.15 mmol) was heated in refluxing toluene (50 mL) for 60 min. The yellow precipitate was collected, washed with copious amounts of ether, and dried under vacuum to provide **3e** as a yellow powder (0.10 g, 54%). A crystal suitable for a single-crystal X-ray diffraction experiment was grown by vapor diffusion of ether into a dichloromethane solution of **3e** at room temperature. Anal. Calcd for $C_{70}H_{52}N_6O_4P_2Ru_2$: C, 64.41; H, 4.02; N, 6.44. Found: C, 64.38; H, 4.08; N, 6.42. ^{1}H NMR (400 MHz, a mixture of $CDCl_3$ and CD_3OD, ppm): 7.41 (d, J = 8.4 Hz, 2H), 7.23 (t, J = 7.6 Hz, 4H), 7.08 (t, J = 6.4 Hz, 8H), 6.96−6.81 (m, 22H), 6.43 (d, J = 8.4 Hz, 2H), 6.37 (d, J = 7.6 Hz, 2H), 6.30 (d, J = 7.2 Hz, 2H), 6.22 (t, J = 7.0 Hz, 2H), 5.74 (d, J = 7.6 Hz, 2H), 5.42−5.36 (m, 4H), 4.50 (s, 2H). ^{31}P NMR (162 MHz, a mixture of $CDCl_3$ and CD_3OD, ppm): 41.2. IR (ν_{CO}, in DCM, cm^{-1}): 1939 (s).

Computational Details. All DFT calculations in this study were performed using the Gaussian 09 suite of programs[26] for the M06 functional[27] in conjunction with an all-electron 6-31G(d) basis set for H, C, N, O, and P atoms. The Stuttgart relativistic effective core potential basis set was used for Ru (ECP28MWB).[28] An ultrafine grid (99,590) was used for numerical integrations. All structures were fully optimized in toluene with solvent effects corrected by using the integral equation formalism polarizable continuum model (IEFPCM)[29] and the SMD radii.[30] Thermal corrections were computed within the harmonic potential approximation on optimized structures at 298.15 K and 1 atm pressure.

■ ASSOCIATED CONTENT

Supporting Information

The Supporting Information is available free of charge on the ACS Publications website at DOI: 10.1021/acs.organomet.8b00432.

Crystallographic details and IR and NMR spectra of the new compounds (PDF)

Calculated absolute energies and atomic coordinates of all optimized structures (XYZ)

Accession Codes

CCDC 1433315−1433316, 1433385, and 1837086 contain the supplementary crystallographic data for this paper. These data can be obtained free of charge via www.ccdc.cam.ac.uk/data_request/cif, or by emailing data_request@ccdc.cam.ac.uk, or by contacting The Cambridge Crystallographic Data Centre, 12 Union Road, Cambridge CB2 1EZ, UK; fax: +44 1223 336033.

■ AUTHOR INFORMATION

Corresponding Authors

*E-mail for X.Y.: xyang@iccas.ac.cn.

*E-mail for D.C.: dafachen@hit.edu.cn.

ORCID

Xinzheng Yang: 0000-0002-2036-1220

Dafa Chen: 0000-0002-7650-4024

Notes

The authors declare no competing financial interest.

■ ACKNOWLEDGMENTS

This work was supported by the National Natural Science Foundation of China (Nos. 21672045, 21702038, and 21673250), the National Science and Technology Pillar Program during the Twelfth Five-Year Plan Period (2015BAD15B0502), the China Postdoctoral Science Foundation (2016M591519), Shenzhen Fundamental research projects (JCYJ20160525164227350, and JCYJ20170811161344569), and the Heilongjiang Postdoctoral Foundation (LBH-Z16069).

■ REFERENCES

(1) For selected reviews, see: (a) Khusnutdinova, J. R.; Milstein, D. Metal-Ligand Cooperation. *Angew. Chem., Int. Ed.* **2015**, *54*, 12236−12273. (b) Zell, T.; Milstein, D. Hydrogenation and Dehydrogenation Iron Pincer Catalysts Capable of Metal-Ligand Cooperation by Aromatization/Dearomatization. *Acc. Chem. Res.* **2015**, *48*, 1979−1994. (c) Morris, R. H. Exploiting Metal-Ligand Bifunctional Reactions in the Design of Iron Asymmetric Hydrogenation Catalysts. *Acc. Chem. Res.* **2015**, *48*, 1494−1502. (d) Li, H.; Zheng, B.; Huang, K. W. A New Class of PN^3-Pincer Ligands for Metal-Ligand Cooperative Catalysis. *Coord. Chem. Rev.* **2015**, *293−294*, 116−138. (e) Younus, H. A.; Su, W.; Ahmad, N.; Chen, S.; Verpoort, F.; et al. Ruthenium Pincer Complexes: Synthesis and Catalytic Applications. *Adv. Synth. Catal.* **2015**, *357*, 283−330. (f) Werkmeister, S.; Neumann, J.; Junge, K.; Beller, M.; et al. Pincer-Type Complexes for Catalytic (De) Hydrogenation and Transfer (De) Hydrogenation Reactions: Recent Progress. *Chem. - Eur. J.* **2015**, *21*, 12226−12250. (g) Kuwata, S.; Ikariya, T. Metal-Ligand Bifunctional Reactivity and Catalysis of Protic N-Heterocyclic Carbene and Pyrazole Complexes Featuring *β*-NH Units. *Chem. Commun.* **2014**, *50*, 14290−14300. (h) Gunanathan, C.; Milstein, D. Bond Activation and Catalysis by Ruthenium Pincer Complexes. *Chem. Rev.* **2014**, *114*, 12024−12087. (i) Zhao, B.; Han, Z.; Ding, K. The N-H Functional Group in Organometallic Catalysis. *Angew. Chem., Int. Ed.* **2013**, *52*, 4744−4788. (j) Warner, M. C.; Bäckvall, J.-E. Mechanistic Aspects on Cyclopentadienylruthenium Complexes in Catalytic Racemization of Alcohols. *Acc. Chem. Res.* **2013**, *46*, 2545−2555.

(2) For selected examples, see: (a) Chakraborty, S.; Leitus, G.; Milstein, D. Iron-Catalyzed Mild and Selective Hydrogenative Cross-Coupling of Nitriles and Amines To Form Secondary Aldimines. *Angew. Chem., Int. Ed.* **2017**, *56*, 2074−2078. (b) Matsunami, A.; Kuwata, S.; Kayaki, Y. A Bifunctional Iridium Catalyst Modified for Persistent Hydrogen Generation from Formic Acid: Understanding Deactivation via Cyclometalation of a 1, 2-Diphenylethylenediamine Motif. *ACS Catal.* **2017**, *7*, 4479−4484. (c) Yuwen, J.; Chakraborty, S.; Brennessel, W. W.; Jones, W. D. Additive-Free Cobalt-Catalyzed Hydrogenation of Esters to Alcohols. *ACS Catal.* **2017**, *7*, 3735−3740. (d) Piehl, P.; Peñalópez, M.; Frey, A.; Neumann, H.; Beller, M. Hydrogen Autotransfer and Related Dehydrogenative Coupling

Reactions Using a Rhenium (I) Pincer Catalyst. *Chem. Commun.* **2017**, *53*, 3265−3268. (e) Nguyen, D. H.; Trivelli, X.; Capet, F.; Paul, J.-F.; Dumeignil, F.; Gauvin, R. M. Manganese Pincer Complexes for the Base-Free, Acceptorless Dehydrogenative Coupling of Alcohols to Esters: Development, Scope, and Understanding. *ACS Catal.* **2017**, *7*, 2022−2032. (f) Chen, X.; Jing, Y.; Yang, X. Unexpected Direct Hydride Transfer Mechanism for the Hydrogenation of Ethyl Acetate to Ethanol Catalyzed by SNS Pincer Ruthenium Complexes. *Chem. - Eur. J.* **2016**, *22*, 1950−1957. (g) Xu, R.; Chakraborty, S.; Bellows, S. M.; Yuan, H.; Cundari, T. R.; Jones, W. D. Iron-Catalyzed Homogeneous Hydrogenation of Alkenes under Mild Conditions by a Stepwise, Bifunctional Mechanism. *ACS Catal.* **2016**, *6*, 2127−2135. (h) Zuo, W.; Prokopchuk, D. E.; Lough, A. J.; Morris, R. H. Details of the Mechanism of the Asymmetric Transfer Hydrogenation of Acetophenone Using the Amine (imine) diphosphine Iron Precatalyst: The Base Effect and The Enantiodetermining Step. *ACS Catal.* **2016**, *6*, 301−314. (i) Nielsen, M.; Alberico, E.; Baumann, W.; Drexler, H.-J.; Junge, H.; Gladiali, S.; Beller, M. Low-Temperature Aqueous-Phase Methanol Dehydrogenation to Hydrogen and Carbon Dioxide. *Nature* **2013**, *495*, 85−89. (j) Rodríguez-Lugo, R. E.; Trincado, M.; Vogt, M.; Tewes, F.; Santiso-Quinones, G.; Grützmacher, H. A Homogeneous Transition Metal Complex for Clean Hydrogen Production from Methanol-Water Mixtures. *Nat. Chem.* **2013**, *5*, 342−347. (k) Otsuka, T.; Ishii, A.; Dub, P. A.; Ikariya, T. Practical Selective Hydrogenation of α-Fluorinated Esters with Bifunctional Pincer-Type Ruthenium (II) Catalysts Leading to Fluorinated Alcohols or Fluoral Hemiacetals. *J. Am. Chem. Soc.* **2013**, *135*, 9600−9603.

(3) For selected examples, see: (a) Dahl, E. W.; Louisgoff, T.; Szymczak, N. K. Second Sphere Ligand Modifications Enable a Recyclable Catalyst for Oxidant-Free Alcohol Oxidation to Carboxylates. *Chem. Commun.* **2017**, *53*, 2287−2289. (b) Gorgas, N.; Alves, L. G.; Stöger, B.; Martins, A. M.; Veiros, L. F.; Kirchner, K. Stable, Yet Highly Reactive Nonclassical Iron (II) Polyhydride Pincer Complexes: Z-Selective Dimerization and Hydroboration of Terminal Alkynes. *J. Am. Chem. Soc.* **2017**, *139*, 8130−8133. (c) Li, H.; Wang, Y.; Lai, Z.; Huang, K.-W. Selective Catalytic Hydrogenation of Arenols by a Well-Defined Complex of Ruthenium and Phosphorus-Nitrogen PN^3-Pincer Ligand Containing a Phenanthroline Backbone. *ACS Catal.* **2017**, *7*, 4446−4450. (d) Deibl, N.; Kempe, R. General and Mild Cobalt-Catalyzed C-Alkylation of Unactivated Amides and Esters with Alcohols. *J. Am. Chem. Soc.* **2016**, *138*, 10786−10789. (e) Chai, H.; Liu, T.; Wang, Q.; Yu, Z. Substituent Effect on the Catalytic Activity of Ruthenium (II) Complexes Bearing a Pyridyl-Supported Pyrazolyl-Imidazolyl Ligand for Transfer Hydrogenation of Ketones. *Organometallics* **2015**, *34*, 5278−5284. (f) Ferrer, Í.; Rich, J.; Fontrodona, X.; Rodríguez, M.; Romero, I. Ru (II) Complexes Containing Dmso and Pyrazolyl Ligands as Catalysts for Nitrile Hydration in Environmentally Friendly Media. *Dalton Trans.* **2013**, *42*, 13461−13469. (g) Bellarosa, L.; Díez, J.; Gimeno, J.; Lledós, A.; Suárez, F. J.; Ujaque, G.; Vicent, C. Highly Efficient Redox Isomerisation of Allylic Alcohols Catalysed by Pyrazole-Based Ruthenium (IV) Complexes in Water: Mechanisms of Bifunctional Catalysis in Water. *Chem. - Eur. J.* **2012**, *18*, 7749−7765.

(4) (a) Toda, T.; Saitoh, K.; Yoshinari, A.; Ikariya, T.; Kuwata, S. Synthesis and Structures of NCN Pincer-Type Ruthenium and Iridium Complexes Bearing Protic Pyrazole Arms. *Organometallics* **2017**, *36*, 1188−1195. (b) Touge, T.; Nara, H.; Fujiwhara, M.; Kayaki, Y.; Ikariya, T. Efficient Access to Chiral Benzhydrols via Asymmetric Transfer Hydrogenation of Unsymmetrical Benzophenones with Bifunctional Oxo-Tethered Ruthenium Catalysts. *J. Am. Chem. Soc.* **2016**, *138*, 10084−10087. (c) Umehara, K.; Kuwata, S.; Ikariya, T. Synthesis, Structures, and Reactivities of Iron, Cobalt, and Manganese Complexes Bearing a Pincer Ligand with Two Protic Pyrazole Arms. *Inorg. Chim. Acta* **2014**, *413*, 136−142. (d) Umehara, K.; Kuwata, S.; Ikariya, T. N-N Bond Cleavage of Hydrazines with a Multiproton-Responsive Pincer-Type Iron Complex. *J. Am. Chem. Soc.* **2013**, *135*, 6754−6757. (e) Yoshinari, A.; Tazawa, A.; Kuwata, P. S.; Ikariya, P. T. Synthesis, Structures, and Reactivities of Pincer-Type Ruthenium Complexes Bearing Two Proton-Responsive Pyrazole Arms. *Chem. - Asian J.* **2012**, *7*, 1417−1425. (f) Kashiwame, Y.; Kuwata, S.; Ikariya, T. Catalytic Intramolecular Hydroamination with a Bifunctional Iridium Pyrazolato Complex: Substrate Scope and Mechanistic Elucidation. *Organometallics* **2012**, *31*, 8444−8455.

(5) Gunanathan, C.; Milstein, D. Metal-ligand Cooperation by Aromatization-Dearomatization: a New Paradigm in Bond Activation and "Green" Catalysis. *Acc. Chem. Res.* **2011**, *44*, 588−602.

(6) For recent examples, see: (a) Espinosa-Jalapa, N. A.; Kumar, A.; Leitus, G.; Diskin-Posner, Y.; Milstein, D. Synthesis of Cyclic Imides by Acceptorless Dehydrogenative Coupling of Diols and Amines Catalyzed by a Manganese Pincer Complex. *J. Am. Chem. Soc.* **2017**, *139*, 11722−11725. (b) Zeng, R.; Feller, M.; Ben-David, Y.; Milstein, D. Hydrogenation and Hydrosilylation of Nitrous Oxide Homogeneously Catalyzed by a Metal Complex. *J. Am. Chem. Soc.* **2017**, *139*, 5720−5723. (c) Xie, Y.; Ben-David, Y.; Shimon, L. J. W.; Milstein, D. Highly Efficient Process for Production of Biofuel from Ethanol Catalyzed by Ruthenium Pincer Complexes. *J. Am. Chem. Soc.* **2016**, *138*, 9077−9080. (d) Nerush, A.; Vogt, M.; Gellrich, U.; Leitus, G.; Ben-David, Y.; Milstein, D. Template Catalysis by Metal-Ligand Cooperation. C-C Bond Formation via Conjugate Addition of Non-activated Nitriles under Mild, Base-free Conditions Catalyzed by a Manganese Pincer Complex. *J. Am. Chem. Soc.* **2016**, *138*, 6985−6997. (e) Feller, M.; Gellrich, U.; Anaby, A.; Diskin-Posner, Y.; Milstein, D. Reductive Cleavage of CO_2 by Metal-Ligand-Cooperation Mediated by an Iridium Pincer Complex. *J. Am. Chem. Soc.* **2016**, *138*, 6445−6454.

(7) (a) Wen, H.; Zhang, L.; Zhu, S.; Liu, G.; Huang, Z. Stereoselective Synthesis of Trisubstituted Alkenes via Cobalt-Catalyzed Double Dehydrogenative Borylations of 1-Alkenes. *ACS Catal.* **2017**, *7*, 6419−6425. (b) Hou, C.; Jiang, J.; Li, Y.; Zhao, C.; Ke, Z. When Bifunctional Catalyst Encounters Dual MLC Modes: DFT Study on the Mechanistic Preference in Ru-PNNH Pincer Complex Catalyzed Dehydrogenative Coupling Reaction. *ACS Catal.* **2017**, *7*, 786−795. (c) Jia, X.; Huang, Z. Conversion of Alkanes to Linear Alkylsilanes Using an Iridium-Iron-Catalysed Tandem Dehydrogenation-Isomerization-Hydrosilylation. *Nat. Chem.* **2016**, *8*, 157−161. (d) Simler, T.; Braunstein, P.; Danopoulos, A. A. Chromium(II) Pincer Complexes with Dearomatized PNP and PNC Ligands: A Comparative Study of Their Catalytic Ethylene Oligomerization Activity. *Organometallics* **2016**, *35*, 4044−4049. (e) Zhang, L.; Zuo, Q.; Leng, X.; Huang, Z. A Cobalt-Catalyzed Alkene Hydroboration with Pinacolborane. *Angew. Chem., Int. Ed.* **2014**, *53*, 2696−2700. (f) Zhang, L.; Peng, D.; Leng, X.; Huang, Z. Iron-Catalyzed, Atom-Economical, Chemo-and Regioselective Alkene Hydroboration with Pinacolborane. *Angew. Chem., Int. Ed.* **2013**, *52*, 3676−3680.

(8) Moore, C. M.; Dahl, E. W.; Szymczak, N. K. Beyond H_2: Exploiting 2-Hydroxypyridine as a Design Element from [Fe]-Hydrogenase for Energy-Relevant Catalysis. *Curr. Opin. Chem. Biol.* **2015**, *25*, 9−17.

(9) (a) Fujita, K.; Tamura, R.; Tanaka, Y.; Yoshida, M.; Onoda, M.; Yamaguchi, R. Dehydrogenative Oxidation of Alcohols in Aqueous Media Catalyzed by a Water-Soluble Dicationic Iridium Complex Bearing a Functional N-Heterocyclic Carbene Ligand without Using Base. *ACS Catal.* **2017**, *7*, 7226−7230. (b) Fujita, K.; Wada, T.; Shiraishi, T. Reversible Interconversion between 2,5-Dimethylpyrazine and 2,5-Dimethylpiperazine by Iridium-Catalyzed Hydrogenation/Dehydrogenation for Efficient Hydrogen Storage. *Angew. Chem., Int. Ed.* **2017**, *56*, 10886−10889. (c) Fujita, K.; Kawahara, R.; Aikawa, T.; Yamaguchi, R. Hydrogen Production from a Methanol-Water Solution Catalyzed by an Anionic Iridium Complex Bearing a Functional Bipyridonate Ligand under Weakly Basic Conditions. *Angew. Chem., Int. Ed.* **2015**, *54*, 9057−9060. (d) Zeng, G.; Sakaki, S.; Fujita, K.; Sano, H.; Yamaguchi, R. Efficient Catalyst for Acceptorless Alcohol Dehydrogenation: Interplay of Theoretical and Experimental Studies. *ACS Catal.* **2014**, *4*, 1010−1020. (e) Fujita, K.; Tanaka, Y.; Kobayashi, M.; Yamaguchi, R. Homogeneous Perdehydrogenation and Perhydrogenation of Fused Bicyclic N-Heterocycles Catalyzed by

DOI: 10.1021/acs.organomet.8b00432
Organometallics XXXX, XXX, XXX−XXX

Iridium Complexes Bearing a Functional Bipyridonate Ligand. *J. Am. Chem. Soc.* **2014**, *136*, 4829−4832. (f) Kawahara, R.; Fujita, K.; Yamaguchi, R. Cooperative Catalysis by Iridium Complexes with a Bipyridonate Ligand: Versatile Dehydrogenative Oxidation of Alcohols and Reversible Dehydrogenation-Hydrogenation between 2-Propanol and Acetone. *Angew. Chem., Int. Ed.* **2012**, *51*, 12790−12794.

(10) (a) Duan, L.; Manbeck, G. F.; Kowalczyk, M.; Szalda, D. J.; Muckerman, J. T.; Himeda, Y.; Fujita, E. Noninnocent Proton-Responsive Ligand Facilitates Reductive Deprotonation and Hinders CO_2 Reduction Catalysis in $[Ru(tpy)(6DHBP)(NCCH_3)]^{2+}$ (6DHBP = 6,6′-$(OH)_2$bpy). *Inorg. Chem.* **2016**, *55*, 4582−4594. (b) Wang, W.-H.; Ertem, M. Z.; Xu, S.; Onishi, N.; Manaka, Y.; Suna, Y.; Kambayashi, H.; Muckerman, J. T.; Fujita, E.; Himeda, Y. Highly Robust Hydrogen Generation by Bioinspired Ir Complexes for Dehydrogenation of Formic Acid in Water: Experimental and Theoretical Mechanistic Investigations at Different pH. *ACS Catal.* **2015**, *5*, 5496−5504. (c) Onishi, N.; Xu, S.; Manaka, Y.; Suna, Y.; Wang, W.-H.; Muckerman, J. T.; Fujita, E.; Himeda, Y. CO_2 Hydrogenation Catalyzed by Iridium Complexes with a Proton-Responsive Ligand. *Inorg. Chem.* **2015**, *54*, 5114−5123. (d) Wang, W.-H.; Muckerman, J. T.; Fujita, E.; Himeda, Y. Mechanistic Insight through Factors Controlling Effective Hydrogenation of CO_2 Catalyzed by Bioinspired Proton-Responsive Iridium(III) Complexes. *ACS Catal.* **2013**, *3*, 856−860. (e) Wang, W.-H.; Hull, J. F.; Muckerman, J. T.; Fujita, E.; Himeda, Y. Second-Coordination-Sphere and Electronic Effects Enhance Iridium(III)-Catalyzed Homogeneous Hydrogenation of Carbon Dioxide in Water Near Ambient Temperature and Pressure. *Energy Environ. Sci.* **2012**, *5*, 7923−7926. (f) Hull, J. F.; Himeda, Y.; Wang, W.-H.; Hashiguchi, B.; Periana, R.; Szalda, D. J.; Muckerman, J. T.; Fujita, E. Reversible Hydrogen Storage Using CO_2 and a Proton-Switchable Iridium Catalyst in Aqueous Media under Mild Temperatures and Pressures. *Nat. Chem.* **2012**, *4*, 383−388.

(11) Siek, S.; Burks, D. B.; Gerlach, D. L.; Liang, G.; Tesh, J. M.; Thompson, C. R.; Qu, F.; Shankwitz, J. E.; Vasquez, R. M.; Chambers, N.; Szulczewski, G. J.; Grotjahn, D. B.; Webster, C. E.; Papish, E. T. Iridium and Ruthenium Complexes of *N*-Heterocyclic Carbene- and Pyridinol-Derived Chelates as Catalysts for Aqueous Carbon Dioxide Hydrogenation and Formic Acid Dehydrogenation: The Role of the Alkali Metal. *Organometallics* **2017**, *36*, 1091−1106.

(12) (a) Chakraborty, S.; Piszel, P. E.; Hayes, C. E.; Baker, R. T.; Jones, W. D. Highly Selective Formation of n-Butanol from Ethanol through the Guerbet Process: A Tandem Catalytic Approach. *J. Am. Chem. Soc.* **2015**, *137*, 14264−14267. (b) Chakraborty, S.; Piszel, P. E.; Brennessel, W. W.; Jones, W. D. A Single Nickel Catalyst for the Acceptorless Dehydrogenation of Alcohols and Hydrogenation of Carbonyl Compounds. *Organometallics* **2015**, *34*, 5203−5206.

(13) Sahoo, A. R.; Jiang, F.; Bruneau, C.; Sharma, G. V. M; Suresh, S.; Roisnel, T.; Dorcet, V.; Achard, M. Phosphine-Pyridonate Ligands Containing Octahedral Ruthenium Complexes: Access to Esters and Formic Acid. *Catal. Sci. Technol.* **2017**, *7* (7), 3492−3498.

(14) Wang, R.; Ma, J.; Li, F. Synthesis of α-Alkylated Ketones via Tandem Acceptorless Dehydrogenation/α-Alkylation from Secondary and Primary Alcohols Catalyzed by Metal-Ligand Bifunctional Iridium Complex $[Cp^*Ir(2,2'\text{-bpyO})(H_2O)]$. *J. Org. Chem.* **2015**, *80*, 10769−10776.

(15) Nieto, I.; Livings, M. S.; Sacci, J. B.; Reuther, L. E.; Zeller, M.; Papish, E. T. Transfer Hydrogenation in Water via a Ruthenium Catalyst with OH Groups near the Metal Center on a bipy Scaffold. *Organometallics* **2011**, *30*, 6339−6342.

(16) Royer, A. M.; Rauchfuss, T. B.; Gray, D. L. Organoiridium Pyridonates and Their Role in the Dehydrogenation of Alcohols. *Organometallics* **2010**, *29*, 6763−6768.

(17) (a) Chakrabarti, K.; Maji, M.; Panja, D.; Paul, B.; Shee, S.; Das, G. K.; Kundu, S. Utilization of MeOH as a C1 Building Block in Tandem Three-Component Coupling Reaction. *Org. Lett.* **2017**, *19*, 4750−4753. (b) Roy, B. C.; Chakrabarti, K.; Shee, S.; Paul, S.; Kundu, S. Bifunctional Ru^{II}-Complex-Catalysed Tandem C-C Bond Formation: Efficient and Atom Economical Strategy for the Utilisation of Alcohols as Alkylating. Agents. *Chem. - Eur. J.* **2016**, *22*, 18147−18155. (c) Chakrabarti, K.; Paul, B.; Maji, M.; Roy, B. C.; Shee, S.; Kundu, S. Bifunctional Ru(II) complex catalysed carbon-carbon bond formation: an eco-friendly hydrogen borrowing strategy. *Org. Biomol. Chem.* **2016**, *14*, 10988−10997. (d) Paul, B.; Chakrabarti, K.; Kundu, S. Optimum Bifunctionality in a 2-(2-Pyridyl-2-ol)-1,10-Phenanthroline Based Ruthenium Complex for Transfer Hydrogenation of Ketones and Nitriles: Impact of the Number of 2-Hydroxypyridine Fragments. *Dalton Trans.* **2016**, *45*, 11162−11171.

(18) (a) Moore, C. M.; Bark, B.; Szymczak, N. K. Simple Ligand Modifications with Pendent OH Groups Dramatically Impact the Activity and Selectivity of Ruthenium Catalysts for Transfer Hydrogenation: The Importance of Alkali Metals. *ACS Catal.* **2016**, *6*, 1981−1990. (b) Tseng, K.-N. T.; Lin, S.; Kampf, J. W.; Szymczak, N. K. Upgrading Ethanol to 1-Butanol with a Homogeneous Air-Stable Ruthenium Catalyst. *Chem. Commun.* **2016**, *52*, 2901−2904. (c) Geri, J. B.; Szymczak, N. K. A Proton-Switchable Bifunctional Ruthenium Complex That Catalyzes Nitrile Hydroboration. *J. Am. Chem. Soc.* **2015**, *137*, 12808−12814. (d) Moore, C. M.; Szymczak, N. K. Nitrite Reduction by Copper through Ligand-Mediated Proton and Electron Transfer. *Chem. Sci.* **2015**, *6*, 3373−3377. (e) Moore, C. M.; Szymczak, N. K. 6,6′-Dihydroxy Terpyridine: a Proton-Responsive Bifunctional Ligand and Its Application in Catalytic Transfer Hydrogenation of Ketones. *Chem. Commun.* **2013**, *49*, 400−402.

(19) (a) Fogler, E.; Garg, J. A.; Hu, P.; Leitus, G.; Shimon, L. J. W.; Milstein, D. System with Potential Dual Modes of Metal-Ligand Cooperation: Highly Catalytically Active Pyridine-Based PNNH-Ru Pincer Complexes. *Chem. - Eur. J.* **2014**, *20*, 15727−15731. (b) Langer, R.; Fuchs, I.; Vogt, M.; Balaraman, E.; Diskin-Posner, Y.; Shimon, L. J. W.; Ben-David, Y.; Milstein, D. Stepwise Metal-Ligand Cooperation by a Reversible Aromatization/Deconjugation Sequence in Ruthenium Complexes with a Tetradentate Phenanthroline-Based Ligand. *Chem. - Eur. J.* **2013**, *19*, 3407−3414.

(20) (a) Toda, T.; Yoshinari, A.; Ikariya, T.; Kuwata, S. Protic N-Heterocyclic Carbene Versus Pyrazole: Rigorous Comparison of Proton- and Electron-Donating Abilities in a Pincer-Type Framework. *Chem. - Eur. J.* **2016**, *22*, 16675−16683. (b) Toda, T.; Kuwata, S.; Ikariya, T. Unsymmetrical Pincer-Type Ruthenium Complex Containing β-Protic Pyrazole and N-Heterocyclic Carbene Arms: Comparison of Brønsted Acidity of NH Groups in Second Coordination Sphere. *Chem. - Eur. J.* **2014**, *20*, 9539−9542.

(21) (a) Tang, Z.; Otten, E.; Reek, J. N. H.; van der Vlugt, J. I.; de Bruin, B. Dynamic Ligand Reactivity in a Rhodium Pincer Complex. *Chem. - Eur. J.* **2015**, *21*, 12683−12693. (b) Tang, Z.; Mandal, S.; Paul, N. D.; Lutz, M.; Li, P.; van der Vlugt, J. I.; de Bruin, B. Rhodium Catalysed Conversion of Carbenes into Ketenes and Ketene Imines Using PNN Pincer Complexes. *Org. Chem. Front.* **2015**, *2*, 1561−1577. (c) de Boer, S. Y.; Korstanje, T. J.; La Rooij, S. R.; Kox, R.; Reek, J. N.; van der Vlugt, J. I. Ruthenium PNN(O) Complexes: Cooperative Reactivity and Application as Catalysts for Acceptorless Dehydrogenative Coupling Reaction. *Organometallics* **2017**, *36*, 1541−1549.

(22) (a) Shi, J.; Hu, B.; Chen, X.; Shang, S.; Deng, D.; Sun, Y.; Shi, W.; Yang, X.; Chen, D. Synthesis, Reactivity, and Catalytic Transfer Hydrogenation Activity of Ruthenium Complexes Bearing NNN Tridentate Ligands: Influence of the Secondary Coordination Sphere. *ACS Omega* **2017**, *2*, 3406−3416. (b) Shi, J.; Hu, B.; Gong, D.; Shang, S.; Hou, G.; Chen, D. Ruthenium Complexes Bearing an Unsymmetrical Pincer Ligand with a 2-Hydroxypyridylmethylene Fragment: Active Catalysts for Transfer Hydrogenation of Ketones. *Dalton Trans.* **2016**, *45*, 4828−4834.

(23) For selected reviews, see: (a) Huang, F.; Liu, Z.; Yu, Z. C-Alkylation of Ketones and Related Compounds by Alcohols: Transition-Metal-Catalyzed Dehydrogenation. *Angew. Chem., Int. Ed.* **2016**, *55*, 862−875. (b) Dobereiner, G. E.; Crabtree, R. H. Dehydrogenation as a Substrate-Activating Strategy in Homogeneous

DOI: 10.1021/acs.organomet.8b00432
Organometallics XXXX, XXX, XXX−XXX

Transition-Metal Catalysis. *Chem. Rev.* **2010**, *110*, 681−703. (c) Nixon, T. D.; Whittlesey, M. K.; Williams, J. M. J. Transition Metal Catalysed Reactions of Alcohols Using Borrowing Hydrogen Methodology. *Dalton Trans.* **2009**, 753−762. (d) Guillena, G.; Ramón, D. J.; Yus, M. Alcohols as Electrophiles in C-C Bond-Forming Reactions: The Hydrogen Autotransfer Process. *Angew. Chem., Int. Ed.* **2007**, *46*, 2358−2364.

(24) (a) Chang, W.; Gong, X.; Wang, S.; Xiao, L. P.; Song, G. Acceptorless Dehydrogenation and Dehydrogenative Coupling of Alcohols Catalysed by Protic NHC Ruthenium Complexes. *Org. Biomol. Chem.* **2017**, *15*, 3466−3471. (b) Wang, Q.; Wu, K.; Yu, Z. Ruthenium(III)-Catalyzed β-Alkylation of Secondary Alcohols with Primary Alcohols. *Organometallics* **2016**, *35*, 1251−1256. (c) Chang, X.; Chuan, L. W.; Li, Y.; Pullarkat, S. A. One-Pot β-Alkylation of Secondary Alcohols with Primary Alcohols Catalyzed by Ruthenacycles. *Tetrahedron Lett.* **2012**, *53*, 1450−1455. (d) Gnanamgari, D.; Sauer, E. L. O.; Schley, N. D.; Butler, C.; Incarvito, C. D.; Crabtree, R. H. Iridium and Ruthenium Complexes with Chelating N-Heterocyclic Carbenes: Efficient Catalysts for Transfer Hydrogenation, β-Alkylation of Alcohols, and N-Alkylation of Amines. *Organometallics* **2009**, *28*, 321−325. (e) Cheung, H. W.; Lee, T. Y.; Lui, H. Y.; Yeung, C. H.; Laua, C. P. Ruthenium-Catalyzed β-Alkylation of Secondary Alcohols with Primary Alcohols. *Adv. Synth. Catal.* **2008**, *350*, 2975−2983. (f) Prades, A.; Viciano, M.; Sanaú, M.; Peris, E. Preparation of a Series of "Ru(*p*-cymene)" Complexes with Different N-Heterocyclic Carbene Ligands for the Catalytic β-Alkylation of Secondary Alcohols and Dimerization of Phenylacetylene. *Organometallics* **2008**, *27*, 4254−4259. (g) Viciano, M.; Sanaú, M.; Peris, E. Ruthenium Janus-Head Complexes with a Triazolediylidene Ligand. Structural Features and Catalytic Applications. *Organometallics* **2007**, *26*, 6050−6054. (h) Martínez, R.; Ramón, D. J.; Yus, M. $RuCl_2(DMSO)_4$, Catalyzes the β-Alkylation of Secondary Alcohols with Primary Alcohols through a Hydrogen Autotransfer Process. *Tetrahedron* **2006**, *62*, 8982−8987.

(25) Jasimuddin, S.; Thakurata, D. G. Synthesis and Characterization of Stable Thiazolylazo Anion Radical Complexes of Ruthenium(II). *Transition Met. Chem.* **2009**, *34*, 937−942.

(26) Frisch, M. J.; Trucks, G. W.; Schlegel, H. B.; Scuseria, G. E.; Robb, M. A.; Cheeseman, J. R.; Scalmani, G.; Barone, V.; Mennucci, B.; Petersson, G. A.; Nakatsuji, H.; Caricato, M.; Hratchian, X. L., H, P.; Izmaylov, A. F.; Bloino, J.; Zheng, G.; Sonnenberg, J. L.; Hada, M.; Ehara, M.; Toyota, K.; Fukuda, R.; Hasegawa, J.; Ishida, M.; Nakajima, T.; Honda, Y.; Kitao, O.; Nakai, H.; Vreven, T.; Montgomery, J. A., Jr.; Peralta, J. E.; Ogliaro, F.; Bearpark, M.; Heyd, J. J.; Brothers, E.; Kudin, K. N.; Staroverov, V. N.; Keith, T.; Kobayashi, R.; Normand, J.; Raghavachari, K.; Rendell, A.; Burant, J. C.; Iyengar, S. S.; Tomasi, J.; Cossi, M.; Rega, N.; Millam, J. M.; Klene, M.; Knox, J. E.; Cross, J. B.; Bakken, V.; Adamo, C.; Jaramillo, J.; Gomperts, R.; Stratmann, R. E.; Yazyev, O.; J. Austin, A.; Cammi, R.; Pomelli, C.; Ochterski, J. W.; Martin, R. L.; Morokuma, K.; Zakrzewski, V. G.; Voth, G. A.; Salvador, P.; Dannenberg, J. J.; Dapprich, S.; Daniels, A. D.; Farkas, O.; Foresman, J. B.; Ortiz, J. V.; Cioslowski, J.; Fox, D. J. *Gaussian 09, revision C.01*; Gaussian, Inc., Wallingford, CT, 2010.

(27) Zhao, Y.; Truhlar, D. G. Theor. Chem. Acc. *Theor. Chem. Acc.* **2008**, *120*, 215−241.

(28) (a) Andrae, D.; Haussermann, U.; Dolg, M.; Stoll, H.; Preuss, H. Energy-Adjusted ab initio, Pseudopotentials for the Second and Third Row Transition Elements. *Theor. Chim. Acta* **1990**, *77*, 123−141. (b) Martin, J. M. L.; Sundermann, A. Correlation Consistent Valence Basis Sets for Use with the Stuttgart-Dresden-Bonn Relativistic Effective Core Potentials: the Atoms Ga-Kr and In-Xe. *J. Chem. Phys.* **2001**, *114*, 3408−3420.

(29) Tomasi, J.; Mennucci, B.; Cammi, R. Quantum Mechanical Continuum Solvation Models. *Chem. Rev.* **2005**, *105*, 2999−3093.

(30) Marenich, A. V.; Cramer, C. J.; Truhlar, D. G. Universal Solvation Model Based on Solute Electron Density and on a Continuum Model of the Solvent Defined by the Bulk Dielectric Constant and Atomic Surface Tensions. *J. Phys. Chem. B* **2009**, *113*, 6378−6396.

DOI: 10.1021/acs.organomet.8b00432
Organometallics XXXX, XXX, XXX−XXX